



Nanoemulsified clove essential oils-based edible coating controls *Pseudomonas* spp.-causing spoilage of tilapia (*Oreochromis niloticus*) fillets: Working mechanism and bacteria metabolic responses

Yaowen Hai^{a,b}, Disheng Zhou^{a,b}, Yi Lin Nicole Lam^a, Xuan Li^{a,b}, Guo Chen^{a,b}, Jintian Bi^{a,b}, Xiaowei Lou^{a,b}, Leijian Chen^{a,b}, Hongshun Yang^{a,b,*}

^a Department of Food Science and Technology, National University of Singapore, Singapore 117542, Singapore

^b National University of Singapore (Suzhou) Research Institute, 377 Lin Quan Street, Suzhou Industrial Park, Suzhou, Jiangsu 215123, PR China

ARTICLE INFO

Keywords:

Nanoemulsion
Essential oil
Edible coating
Pseudomonas spp.
Defense system
NMR
Metabolomics

ABSTRACT

Fish products suffer *Pseudomonas*-causing spoilage quickly during refrigeration storage, which could be solved by applying edible coating derived from nanoemulsified clove essential oils and fish gelatin (NCEO-FG). This study aimed to evaluate the effects and mechanism of NCEO-FG in preserving tilapia (*Oreochromis niloticus*) fillets that were inoculated with *Pseudomonas* spp. (*Pseudomonas* sp. strain ABA3, *P. psychrophila* strain ABE3, and *P. fragi* strain BBa3). NCEO caused remarkable leakage of proteins (183.8–273.7 µg/L) and nucleic acids (0.30–0.34 of OD260). After being incorporated into FG, NCEO-FG effectively delayed the deterioration of tilapia fillets because it significantly reduced the surviving bacteria populations (0.78 – 1.80 log CFU/g reductions) and inhibited the proteolysis and oxidation during cold storage. Further, the metabolic responses of NCEO-FG coated *Pseudomonas* spp. were revealed using NMR spectroscopy: the reducing levels of metabolites (e.g., pyruvate, amino acids, and betaine) suggested that the NCEO-FG disturbed energy and amino acid metabolisms of bacteria cells. However, the levels of metabolites (e.g., amino acids and osmoprotectants) were upregulated after 3 h and then back to normal concentration after 24 h, which indicated a defense system was built in bacterial cells to tolerate NCEO-FG. In short, this study confirmed that NCEO-FG could control the *Pseudomonas*-causing spoilage in fish fillets via elucidating the metabolisms.

1. Introduction

Meat of healthy fish is usually regarded as sterile. However, because of the high content of nutrients and fragile texture, fish meat is favored by spoilage microorganisms that can be introduced into fish products anytime during production and transportation (Sheng & Wang, 2021). Namely, additional processes like filleting can increase the contamination risk and further reduce the shelf life of fish products (Taliadourou, Papadopoulos, Domvridou, Savvaidis, & Kontominas, 2003).

As the major spoilage microorganism in tilapia fillets, *Pseudomonas* adversely affects the quality attributes and thus causing massive spoilage of fish meat during refrigeration storage (Caldera et al., 2016). *Pseudomonas* can even bring safety concerns as it may produce histamine (Sheng & Wang, 2021) and its biofilm provides a protection effect for pathogenic *E. coli* under refrigeration conditions (Sterniša, Klančnik, & Smole Možina, 2019). However, *Pseudomonas* is not easy to be

eliminated as it can withstand various external stresses. Just as Nikel et al. (2021) reported, the redistribution of carbon fluxes in metabolic pathways endows *P. putida* with the capacity to defeat oxidative stress. Moreover, *Pseudomonas* is able to tolerate osmotic pressure because of the additional transporters that can effectively transport osmoprotectants from the environment (Chen, Malek, Wargo, Hogan, & Beattie, 2010). Therefore, more effective agents are needed to control the growth of *Pseudomonas* spp. to preserve perishable food.

As generally recognized as safe (GRAS) substances, plants-derived essential oils (EOs) have long been used in food, medicine, and cosmetics, which can be promising agents to inhibit *Pseudomonas* in food-stuffs, especially clove essential oil (CEO) that has been confirmed with excellent antimicrobial and antioxidant capacities (Fu et al., 2007; Khorshidian, Yousefi, Khanniri, & Mortazavian, 2018). However, EOs cannot be used directly because of the high volatility, which can be solved by being encapsulated into biodegradable materials (Gagaoua

* Corresponding author at: Department of Food science and Technology, National University of Singapore, Singapore 117542, Singapore.

E-mail address: fstynghs@nus.edu.sg (H. Yang).

et al., 2021; Wu, Richards, & Undeland, 2022). Previous studies have already reported that edible coatings derived from nanoemulsified CEO (NCEO) could extend the shelf life of perishable food effectively (Liu et al., 2020; Nisar et al., 2019; Vieira et al., 2019).

However, the knowledge of the working mechanism of NCEO coating and the stress responses of *Pseudomonas* on coated foodstuffs are quite limited, which could be revealed by examining the metabolic alternations from the molecular aspect. Therefore, nuclear magnetic resonance (NMR) spectroscopy was employed in this study as previous studies confirmed that NMR was able to provide qualitative and quantitative information about the *vivo* metabolites of bacteria in complex food matrices (Chen et al., 2020; Chen, Zhao, Li, & Yang, 2022; Wang, Wu, & Yang, 2022; Wu, Zhao, Lai, & Yang, 2021).

This study was realized to evaluate the mechanism of NCEO-encapsulated edible coating in preserving the tilapia fillets inoculated with *Pseudomonas* spp. strains. Specifically, one- and two-dimensional NMR spectra were employed to investigate metabolic responses of *Pseudomonas* spp. on the molecular level. More importantly, the vital pathways identified would provide a helpful guide to better control *Pseudomonas* spp. in other perishable foods.

2. Materials and methods

2.1. Preparation of culture

Three strains of *Pseudomonas* spp. (*Pseudomonas* sp. strain ABa3, *P. psychrophila* strain ABe3, and *P. fragi* strain BBa3) (Fig. S1) cultures were isolated from spoiled golden pomfret fillets. The cryopreserved strains were restored and recultured in Luria-Bertani (LB) Broth at 22 °C.

2.2. Preparation of NCEO-FG coating solution

According to Guo et al. (2020) and Ji et al. (2021) with modifications, an aqueous mixture of Tween 80 (0.3% w/v), CEO (2% w/v), and corn oil (0.8 % w/v) were homogenized (12,000 rpm, 3 min) to form a coarse emulsion. High power ultrasound (20 kHz, 500 W) was then applied (6 s on and 24 s off for 10 min) to form NCEO. Fish gelatin (FG) was added to NCEO till the final concentration achieved 3 g / 100 mL water. After being stirred for 15 min at 45 °C, glycerol (30% of the gelatin mass) was added and stirred continuously for another 30 min. The coating solution was then cooled down for later usage.

2.3. Measurement of CEO and NCEO compositions

According to the method reported by Rezaei & Shahbazi (2018), the compositions of CEO and NCEO were measured using GC-MS (Agilent Scientific Instruments, California, USA) equipped with a HP-5MS 5% phenylmethylsiloxane capillary column (30 m × 0.25 mm × 0.25 µm). The temperature of the oven was initially maintained at 60 °C for 3 min followed by being increased to 300 °C at the rate of 5 °C/min and maintained for 54 min. As for the injection inlet and detector, their temperatures were set at 250 °C. The flow rate and split ratio of helium with 99% purity were set at 1 mL/min and 1:20, respectively. The electron ionization mode of MS was set at 70 eV.

2.4. Investigation of cell-membrane integrity

The membrane integrity was evaluated according to the concentrations of cell constituents in the supernatant after being treated by NCEO at the minimum inhibitory concentration (MIC). The test was designed based on Moghimi, Ghaderi, Rafati, Aliahmadi, & McClements (2016) and Zhao, Chen, Wu, He, & Yang (2020) with modifications. Briefly, the bacteria cells of the three strains were collected, washed, and re-suspended in 0.5 mL of PBS buffer, where the concentration of bacteria cells was 12 log CFU/mL to obtain enough leakage contents. The cell suspension was then mixed with another 4.5 mL of diluted NCEO to

ensure the final concentration of CEO in the mixture was 0.5% w/v (MIC). PBS buffer (5 mL) with bacteria cells and 5 mL of NCEO (0.5% w/v) solution without bacteria cells were employed as two control groups. After 1-hour incubation, the aqueous mixtures were centrifuged at 4,000 × g for 10 min (to prevent leakage caused by high-speed centrifugation) and filtered with a microporous membrane (0.22 µm).

To measure the leakage of protein, 100 µL of supernatant was incubated with equivalent Bradford reagent for 5 min followed by reading the absorbance at 595 nm using a Plate reader (Agilent Scientific Instruments, California, USA). Bovine Serum Albumin (BSA) was employed as standard. As for the evaluation of nucleic acid leakage, 100 µL of supernatant was diluted for 100 times followed by reading the absorbance at 260 nm. The results were shown after subtracting the values of two controls.

2.5. Coating inoculated tilapia fillets

Tilapia (*Oreochromis niloticus*) were purchased from a local supermarket (Fairprice) in Singapore. Sterile fillets (3.0 ± 0.1 g) from the back portion of fish were prepared according to Lou et al. (2021). Each of the three strains was carried out individually. The cultures (10⁸ CFU/mL) were centrifuged, washed, and re-suspended in equivalent peptone water. After dilution, the inocula were inoculated on sterile fish fillets by spotting 50 µL on two sides. After being air-dried for 15 min, the inoculated fillets were stored at 4 °C for 12 h to ensure that the strains were adapted to growing on fish fillets. The final cell concentrations of *Pseudomonas* spp. were 6.5 and 3.5 log CFU/g before treatments, respectively. The inoculated fillets were randomly divided into 4 batches and treated with NCEO-FG (2% w/v of CEO and 3% w/v of FG), NCEO (2% w/v of CEO), water, and FG (3% w/v), respectively. Fillets were dripped into treatment solutions for 1 min and taken out to get air-dried for 2 min followed by another 2 min of recoating. The treated fillets were stored at 4 °C for further analysis.

2.6. Evaluation of antimicrobial effects on fillets

Antimicrobial effects were evaluated based on total viable counts (TVC) of *Pseudomonas* spp. on LB agar plate after treatment. Each coated fillet was homogenized with peptone water (27 mL, 0.1% w/v) for 90 s. After being subjected to serial dilutions, 100 µL of diluent was spread on the LB agar plate and incubated at 23 °C for 48 h. TVC was examined at 0, 3, 24, 72, and 120 h after coating treatment.

2.7. Evaluation of fish deterioration

To mimic the real condition, fillets employed in this part were inoculated with the mixture of the three strains following the same procedures in 2.5. The method of Sobieszczkańska et al. (2020) was applied to evaluate the degree of proteolysis based on the concentration of amino acids in fillets. After being fully homogenized with PBS (10 mL) and centrifuged (12,000 × g, 10 min), the supernatant was collected and filtered with a 0.22-µm microporous membrane. After being diluted for 10 times, 50 µL of supernatant was added into a 96-well plate, which was followed by 100 µL of PBS buffer and 50 µL of 2,4,6-trinitrobenzene sulfonic acid (0.03% w/v) successively. The absorbance was read at 450 nm after 20-min incubation. Leucine was utilized as standard, and the results were presented in the form of mg/g of fish.

Malondialdehyde (MDA) is one product of fatty acids peroxidation, and thus its level can indicate the degree of lipid oxidation in samples. Treated fillets were homogenized with 6 mL of cold trichloroacetic acid (TCA) solution following the same procedures reported by Vital et al. (2018). The concentration of MDA was calculated based on a standard curve constructed by 1,3,3-tetramethoxypropane, and the final results were expressed as µg MDA/kg of fish.

The measurement was conducted before and 0, 3, 24, 72, and 120 h after treatment. The percentage inhibition (PI) of proteolysis and lipid

oxidation was calculated by using the equation below:

$$PI\% = \left(1 - \frac{C_{NCEO}}{C_{water}}\right) \times 100\%$$

Where:

C_{NCEO} : concentration of amino acids or MBA in NCEO-coated fillets.

C_{water} : concentration of amino acids or MBA in water-treated fillets.

2.8. Extraction of metabolites in bacterial cells

The three strains were carried out individually. The extracts were prepared according to Wu et al. (2021) with modifications. In order to obtain analyzable information about metabolites in bacteria cells, one kilogram of fillet was used in each treatment. The inoculated fillets were randomly divided into 4 batches that were before (I) and 0 min (II), 3 h (III), and 24 h (IV) after NCEO-FG coating. After treatment, fillets were fully homogenized and centrifuged twice at $1400 \times g$ for 2 min to completely precipitate fish debris, and the upper clean portion was collected and centrifuged at $12,000 \times g$ for 10 min to obtain *Pseudomonas* spp. cells. The pelleted cells were suspended in a 5 mL extraction solution (NaH₂PO₄–K₂HPO₄ buffer: methanol = 1:1) and sonicated at 500 W for 10 min (6 s on and 24 s off). The mixture was placed at 4 °C for 12 h and centrifuged ($12,000 \times g$, 10 min, 4 °C) to collect the supernatant, which was then placed into a 100 mL round flask. Another 5 mL of extraction solution was added to the cell residues to collect the secondary supernatant. The metabolites were collected after removing water and methanol from combined supernatants using rotary evaporation at 40 MPa and 40 °C. After being dissolved in 700 µL of deuterium oxide (D₂O, 99.9%) containing 0.684 mol/L TSP, 600 µL of the solution was subjected into NMR tubes for further analysis.

2.9. NMR analysis and spectral processing

The detailed operation was performed according to Lou et al. (2021). One- and two-dimensional NMR spectra were performed on a Bruker AV-500 NMR Spectrometer (Bruker Biospin, Rheinstetten, Germany). The spectra of ¹H (10 ppm) and ¹³C (160 ppm) were imported in TopSpin 3.6.3 (Bruker) to do manual adjustment (e.g., baseline, TSP signal, and phase). The identification of metabolites was conducted using the two-dimensional NMR spectra and metabolomic databases, including Human Metabolome Database (HMDB) and Biological Magnetic Resonance Data Bank (BMRB). In MestreNova (Mestrelab, Research SL, Santiago de Compostela, Spain), the ¹H spectra excluded regions of solvent (4.70–4.80 ppm) and methanol (3.33–3.38 ppm) was binned into 0.01 ppm and exported for further analysis.

The signals without overlapping peaks were selected and quantified based on the TSP peak. The quantification of the identified metabolites was plotted into a heatmap using ClustVis. The alternations of the metabolic profile were examined using principal component analysis (PCA) and orthogonal partial least squares discriminant analysis (OPLS-DA) in SIMCA (version 14.1, Umetrics, Umeå, Sweden). The metabolites with $P < 0.05$ and VIP value > 1 were considered crucial, followed by the identification of crucial pathways performed in MetaboAnalyst 5.0.

2.10. Statistical analysis

All of the experiments were performed in triplicate. Duncan's new multiple range test (MRT), one-way analysis of variance (ANOVA), and Independent Samples t Test were conducted by SPSS software (SPSS, Inc., Chicago, IL) to identify the significant difference. Differences with $P < 0.05$ were considered significant.

3. Results and discussion

3.1. Compositions of CEO and NCEO

The components that accounted for >99% of total content in CEO and NCEO are listed in Table 1. It indicated that eugenol was the major bioactive component in CEO (93.8%) and NCEO (93.6%), which was confirmed with excellent antimicrobial capacity through damage of bacteria membranes, production of intracellular ROS, and inhibition of enzymatic activity (Marchese et al., 2017). Caryophyllene was a minor constituent, which was reported with selective antibacterial capacity against *S. aureus* (Dahham et al., 2015). The slight differences in compositions between NCEO and CEO could be caused by the variation of volume, loss of volatile components, and formation of new compounds during nanoemulsion preparation (Baranauskienė, Bylaitė, Žukauskaitė, & Venskutonis, 2007).

3.2. Leakage of protein and nucleic acid

This part aimed to investigate the capacity of stable NCEO (Fig. S2) in membrane damage. The results subtracted values of controls are shown in Fig. 1. Proteins (198.5–252.8 µg/L) and nucleic acids (0.30–0.34 of OD₂₆₀) were significantly released after being treated by diluted NCEO, which indicated that NCEO could damage the cell membranes of *Pseudomonas* spp., which was consistent with the results of Devi, Nisha, Sakthivel, & Pandian (2010).

Eugenol directly disturbed the lipid profile of the cell membrane and thus altering its non-specific permeability, which was followed by cellular-contents leakage and even cell death (Devi et al., 2010; Di Pasqua, Hoskins, Betts, & Mauriello, 2006). Moreover, a remarkable increase in reactive oxygen species (ROS) levels was observed in various bacterial cells after being treated with eugenol, which aggravated the damage to cell integrity and nucleic acid (Fu et al., 2022).

3.3. Antimicrobial effects of NCEO-FG on fillets

The antimicrobial effects at two inoculation levels (6.5 and 3.5 log CFU/g) were evaluated based on the reduction of the surviving populations after treatment, and the excess of 7 log CFU/g was considered as spoilage (Ellis & Goodacre, 2001). In Fig. 2, lines represented FG and water were always located at the highest portion, and FG even showed worse capacity in controlling *Pseudomonas* spp. at higher inoculation level. NCEO demonstrated significant antimicrobial capacity at the beginning, but it lost this advantage gradually during refrigeration storage because of its volatility.

NCEO-FG coated fillets always showed the lowest TVC during storage. The surviving populations of three strains on coated fillets were significantly reduced after NCEO-FG coating both at high (0.78 to 1.8 log CFU/g reductions) and low (0.87 to 1.37 log CFU/g reductions) inoculation levels. The surviving populations of bacteria cells were gradually recovered after then, which might be resulted from an unknown defense system developed in cells. ABa3 and ABe3 were relatively more sensitive to NCEO-FG as their surviving populations were lower than BBa3 after treatment. Even though BBa3 had higher resistance, NCEO-FG still could extend the shelf-life of fillets for two more

Table 1

The main components in clove essential oil (CEO) and it derived nanoemulsion (NCEO) using GC–MS.

Peak	Retention time (min)	Molecular weight (g/mol)	Compound identified	Percentage in CEO (%)	Percentage in NCEO (%)
1	19.273	164.08	Eugenol	93.8 ± 0.7	93.6 ± 0.3
2	20.584	204.19	Caryophyllene	4.9 ± 0.5	5.6 ± 0.2
3	21.247	136.12	α-Ocimene	/	0.8 ± 0.1
4	21.346	204.19	Humulene	0.8 ± 0.1	/

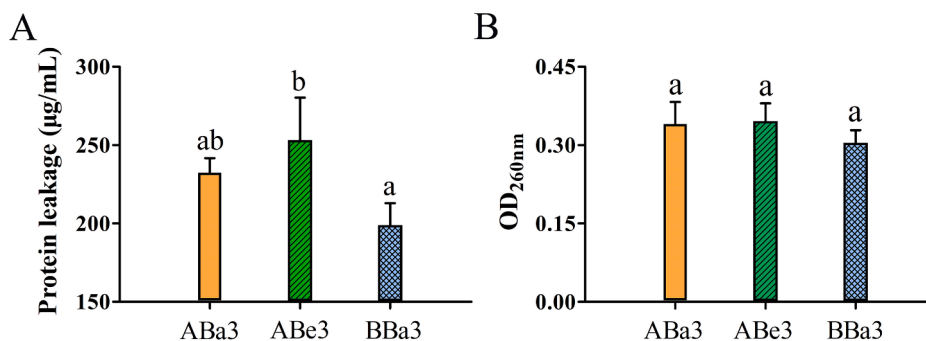


Fig. 1. The leakage of protein (A) and nucleic acid (B) from 3 strains of *Pseudomonas* cells (ABA3, ABe3, and BBA3) after being treated with NCEO for 60 min at MIC (Mean \pm SD, n = 3). Note: The results were showed after subtracting the values of controls; NCEO: nanoemulsified clove essential oil; ABA3: *Pseudomonas* sp. strain; ABe3: *P. psychrophila* strain; BBA3: *P. fragi* strain. Mean values labeled with different lowercase letters are significantly different from the others ($P < 0.05$).

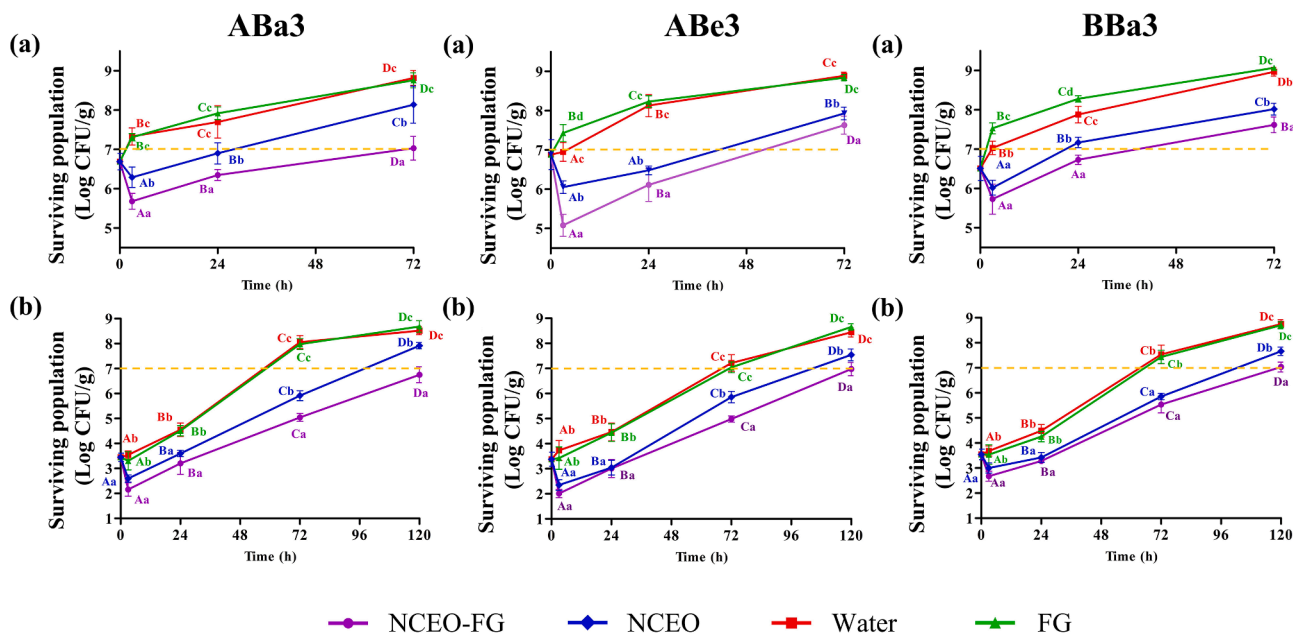


Fig. 2. The surviving populations of ABA3, ABe3 and BBA3 inoculated at 6.5 log CFU/g (a) and 3.5 log CFU/g (b) on tilapia fillets that treated with NCEO-FG, NCEO, water, and FG during storage at 4 °C after treatment (Mean \pm SD, n = 3). Note: NCEO: nanoemulsified clove essential oil; FG: fish gelatin; NCEO-FG: coating based on nanoemulsified clove essential oil and fish gelatin; ABA3: *Pseudomonas* sp. strain; ABe3: *P. psychrophila* strain; and BBA3: *P. fragi* strain. Different uppercase letters represent a significant difference among samples of the same treatment at different storage periods ($P < 0.05$); different lowercase letters represent a significant difference among samples of different treatments at the same storage period ($P < 0.05$).

days than the control at the low inoculation level. Therefore, the cooperation of NCEO and FG contributed to the excellent antimicrobial effects.

The worse performance of FG could be ascribed to the high nutrient contents (e.g., crude protein, minerals, carbohydrates, and water), which provided a more ideal environment for microbial growth (Lv et al., 2019). In NCEO-FG, eugenol could be retained in polymer chains of FG for a longer time, because a large intermolecular force was formed between the hydroxy groups of eugenol and amino acid residues of FG (Wu, Sun, Guo, Ge, & Zhang, 2017). A similar result was reported by Ma et al. (2016) that encapsulation could significantly save the loss of cinnamon bark oil during storage. The study of Sessa, Ferrari, & Donsi (2015) found that nano-encapsulated EOs could extend the shelf-life of ready-to-eat vegetables and fruits up to 7 days. Besides, nano-encapsulated *Ferulago angulata* EO was able to maintain low TVC of psychrotrophic bacteria after 16-day storage at 4 °C (Shokri, Parastouei, Taghdir, & Abbaszadeh, 2020).

3.4. Deterioration of fish fillets within 5-day storage

During storage, the fish meat inevitably suffers deterioration of quality attributes. The proteases and lipases from fish meat and microorganisms attribute to the development of soft texture and undesirable flavor in fish products, which should be slowed down to preserve the quality attributes to the extent possible (Secci & Parisi, 2016).

The amino acid concentrations and TBA values in fillets treated with NCEO-FG and water are shown in Table 2. In the beginning, no significant difference was brought by treatment. Amino acid concentrations and TBA values of NCEO-FG treated fillets were maintained at around 9 mg/g and 69 µg MDA/kg during the first three hours, and gradually increased to 21.4 mg/g and 167.2 µg MDA/kg after 5 days. The amino acid concentrations and TBA values in control groups were significantly higher than in NCEO-coated groups during storage. Moreover, the prohibition effect (PI) of proteolysis in fillets coated with NCEO-FG was the highest (32.9%) at 3 h and then decreased to 18.2% at 24 h. The PI of lipid oxidation shared a similar trend except that the PI rose to the peak (64.1%) at 24 h. The PI was continuously reducing after 24 h, but the

Table 2
The situation of proteolysis and lipid oxidation in tilapia fillets treated with NCEO-FG and water within 5-day storage.

Period (h)	Proteolysis (mg/mL)			TBA (µg MDA/kg)		
	NCEO-FG	Water	PI (%)	NCEO-FG	Water	PI (%)
BT	9.0 ± 0.8 ^{Aa}	9.0 ± 0.8 ^{Aa}	–	68.6 ± 13.8 ^{Aa}	68.6 ± 13.8 ^{Aa}	–
AT 0	8.7 ± 0.8 ^{Aa}	9.9 ± 1.0 ^{Ba}	11.4 ± 8.4 ^{ab}	67.5 ± 18.1 ^{Aa}	68.9 ± 18.8 ^{Aa}	2.1 ± 2.7 ^a
	9.1 ± 0.6 ^{Aab}	13.6 ± 0.2 ^{Bb}	32.9 ± 0.9 ^c	70.5 ± 11.6 ^{Aa}	86.2 ± 9.6 ^{Ba}	18.3 ± 9.8 ^b
24	12.5 ± 0.3 ^{Ab}	15.3 ± 0.5 ^{Bc}	18.2 ± 2.9 ^b	75.8 ± 22.0 ^{Aa}	226.8 ± 59.9 ^{Bb}	64.1 ± 15.6 ^d
	16.5 ± 0.7 ^{Ac}	17.5 ± 0.1 ^{Bd}	5.5 ± 0.4 ^a	134.2 ± 18.0 ^{Ab}	250.2 ± 49.5 ^{Bb}	45.1 ± 9.4 ^c
72	21.4 ± 0.3 ^{Ad}	23.6 ± 0.1 ^{Be}	9.1 ± 0.3 ^a	167.2 ± 39.9 ^{Ab}	263.0 ± 76.1 ^{Bb}	33.7 ± 18.1 ^c

Note: BT: before treatment; AT: after treatment; NCEO-FG: coating based on nanoemulsified clove essential oil and fish gelatin; PI: percentage inhibition. Different uppercase letters in the same row represent a significant difference among samples of different treatments at the same storage period ($P < 0.05$); different lowercase letters in the same columns represent a significant difference among samples of the same treatment at different storage periods ($P < 0.05$).

fillets coated with NCEO-FG showed significantly delayed proteolysis and lipid oxidation till the end of storage.

The cooperation of NCEO and FG contributed to the excellent

capacity in preserving the quality attributes of fillets. On the one hand, FG acted as an effective barrier and reduced the loss of bound water, which could stabilize myofibrils during storage (Ruttanapornvareesakul et al., 2005). Besides, FG reduced the exposure of oxygen, which largely protected unsaturated fatty acids from oxidation (Liu et al., 2012). On the other hand, NCEO could reduce the protease and lipase secreted from bacteria. Just as Sobieszcańska et al. (2020) found, Tarragon EO could suppress the expression of protease-encoding genes in food-associated *Pseudomonas*, and NCEO might have a similar effect. Moreover, the growth of *Pseudomonas* spp. was effectively controlled by NCEO-FG (Fig. 2) so that the total enzymes from bacteria would be reasonably less than the controls. Similar inhibition effects of other edible coatings were reported by Feng, Bansal, & Yang (2016), Yu et al. (2018), and Ojagh, Rezaei, Razavi, & Hosseini (2010).

3.5. Twenty-four-hour metabolic profile of *Pseudomonas* on coated fillets

3.5.1. Heatmap of metabolic alternation within 24 h

Based on the results of 3.3, the surviving populations of *Pseudomonas* spp. were significantly reduced after treatment and gradually recovered within 24 h (Fig. 2), which suggested that bacteria cells might develop a certain defense system to tolerate the stressful environment. Therefore, in order to better control *Pseudomonas* spp., the metabolic changes during this period were worthwhile to be investigated. After NMR spectr3), a total of 45 metabolites from 5 groups (viz, amino acids, carbohydrates, nucleotides, organic acids, and others) were identified (Table S1), quantified (Table S2), and visualized (Fig. 3). The color of blocks in Fig. 3 reflected the levels of metabolites: the reddish and bluish ones represented the high and low concentrations, respectively.

All of the three strains developed similar trends of overall metabolic alternation within 24 h. No visible change in colors existed between

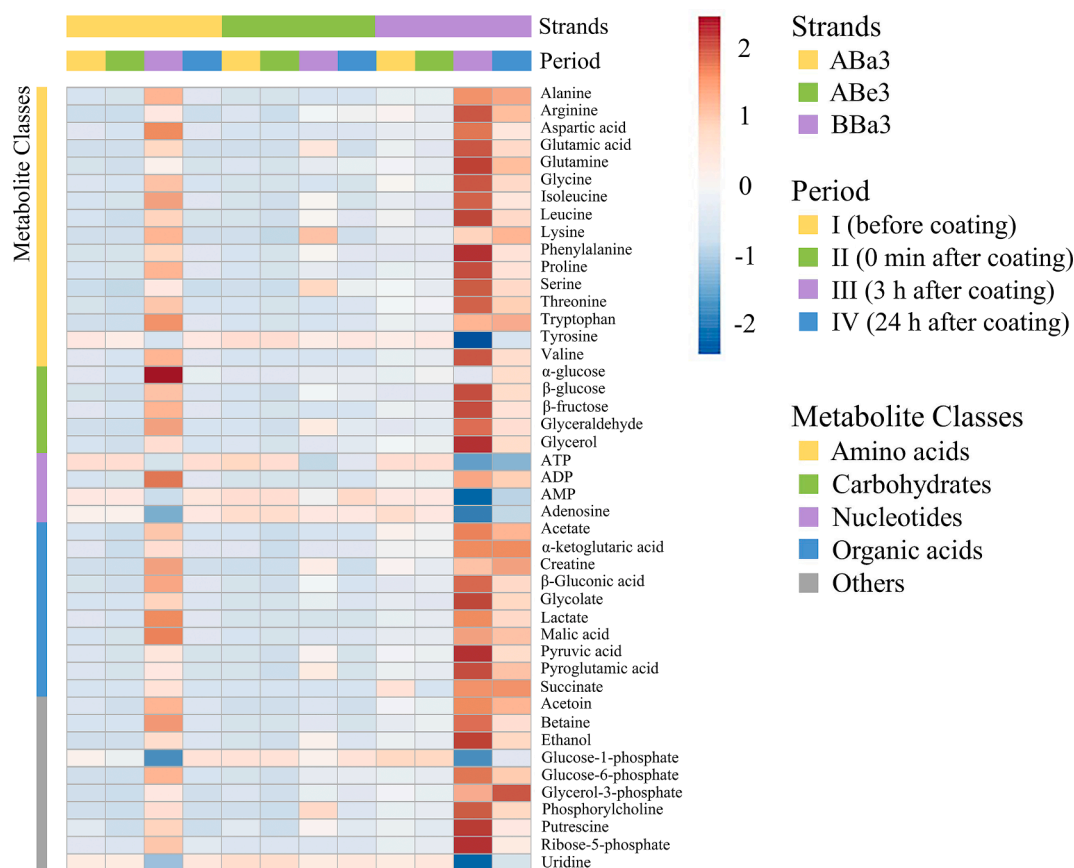


Fig. 3. Heatmaps of metabolites in ABA3, ABe3, and BBa3 on NCEO-FG coated tilapia fillets within 24 h. Note: NCEO-FG: coating based on nanoemulsified clove essential oil and fish gelatin; ABA3: *Pseudomonas* sp. strain; ABe3: *P. psychrophila* strain; and BBa3: *P. fragi* strain.

periods I and II. However, the alternations were noticeable at 3 h (III) that most of the levels of identified metabolites were largely increased, especially amino acids (e.g., Glu, Lys, and Ser), intermediates of energy metabolism (e.g., ethanol and pyruvic acid), and membrane-associated compounds (e.g., phosphorylcholine) while several exceptions like nucleotides (e.g., ATP, AMP, and Adenosine), tyrosine, and uridine demonstrated visible reductions in levels. The reddish colors faded at 24 h (IV), and the differences between periods I and IV were even undetectable in ABa3 and ABe3. Besides slight differences, the color alternations of the three strains suggested that the bacterial cells suffered gradual recovery during 3 to 24 h.

3.5.2. Multivariate analysis of metabolic alternation within 24 h

PCA was employed to unbiasedly demonstrate the inter-correlation of ^1H NMR spectra among ABa3, ABe3, and BBa3. In Fig. 4, PC1 and PC2 explained 94% of the total variance with Q^2 of 0.83, which suggested the model showed satisfying interpretability and predictability (Zhao et al., 2020). The points which represented the metabolic profiles of periods I and II were closely located in the third quadrant. The metabolic trajectories of ABa3 and BBa3 then migrated longer distances along the positive PC1-axis than ABe3 within 3 h (III). After that, ABa3 and ABe3 were back to the third quadrant while BBa3 was not fully recovered at the end of period IV. As reported by Ye et al. (2012), metabolic pathways were regulated precisely for bacteria cells to respond to external stresses. Namely, the magnitude of metabolic alternation might indicate the integrality of the defense system built in cells, and the ones with less change might obtain lower surviving populations after NCEO-FG coating, which was consistent with the results in 3.3.

OPLS-DA with powerful prediction ability was employed to identify the most influential metabolites via pairwise comparison. Because of the high similarity, BBa3 with higher resistant capacity was selected to present the results of OPLS-DA and pathway analysis as shown below (Fig. 5), and the results of the other two strains could be found in Table S3 and S4. OPLS-DA was conducted to compare the data of periods I with II, III, and IV, respectively. According to values of R^2X and Q^2 (Fig. 5A a, c, e), the discriminations between these 4 periods were valid. In the S-line (Fig. 5A b, d, f), p(ctr)[1] on the left y-axis indicated the decreasing or increasing alternations of metabolites while p(corr) on the right side represented the correlation coefficient. The color reliably indicated the correlation with the significance of metabolites, and the red ones indicated the metabolites located were significant (Bervoets et al., 2017). All of the metabolites identified as important in Table S3

were represented in red in S-line figures. Eleven important metabolites with significant reductions were identified between periods I and II, including five amino acids (e.g., Arg and Gln), four intermediates of energy metabolism (e.g., pyruvate & Ribose-5-phosphate), and cell wall-associated constituents (e.g., phosphorylcholine). These results suggested the energy metabolic pathways were disturbed by NCEO. Twenty-two metabolites were significantly affected via comparison of periods I and III, which indicated a high-magnitude alternation of metabolic profile. Among them, amino acids (e.g., Pro, Val, and Phe) and organic acids (e.g., lactate) were remarkably accumulated in bacteria cells. Moreover, the stacks of glycolytic intermediates like G-6-P might indicate the glycolysis was hampered, which were coincided with the depletion of ATP. As for the comparison of periods I and IV, only two important metabolites were identified, which suggested that the BBa3 was capable of tolerating the stressful environments after 24 h.

3.5.3. Pathway analysis

The pathway analysis was conducted based on the metabolites identified as important from OPLS-DA. The important pathways ($-\log(p) > 1.301$ and pathway impact > 0.1) were listed in Table S4 and visualized in Fig. 5B (Guo & Tao, 2018; Wang et al., 2022). Amino acid metabolism contributed largely to the overall metabolic networks. After coating (II), four metabolic pathways related to amino acids were disturbed by NCEO-FG, and this disturbance lasted for 3 h except for the Val, Leu & Ile biosynthesis. The significant influence of NCEO-FG on tyrosine metabolism was observed both at 3 and 24 h. Besides, energy metabolism (e.g., starch & sucrose metabolism and pentose phosphate pathway) also played important role in the overall metabolic networks. The number of metabolic pathways with significant alternation was the least at 24 h, which suggested the bacteria cells were gradually recovered after making a series of metabolic alternations. Therefore, the metabolism related to these two aspects was focused on in the following discussion part.

In order to visualize the alternations in detail, a schematic of important metabolites and metabolic pathways in three strains was plotted (Fig. 6), where the directions of arrows indicated the changes in metabolite levels after NCEO-FG coating.

3.6. Discussion of metabolic alterations under NCEO-FG

The working mechanism of NCEO-FG and the metabolic responses of bacteria cells during the first 24 h were summarized in a schematic diagram (Fig. 7). Three strategies developed by *Pseudomonas* spp. cells to

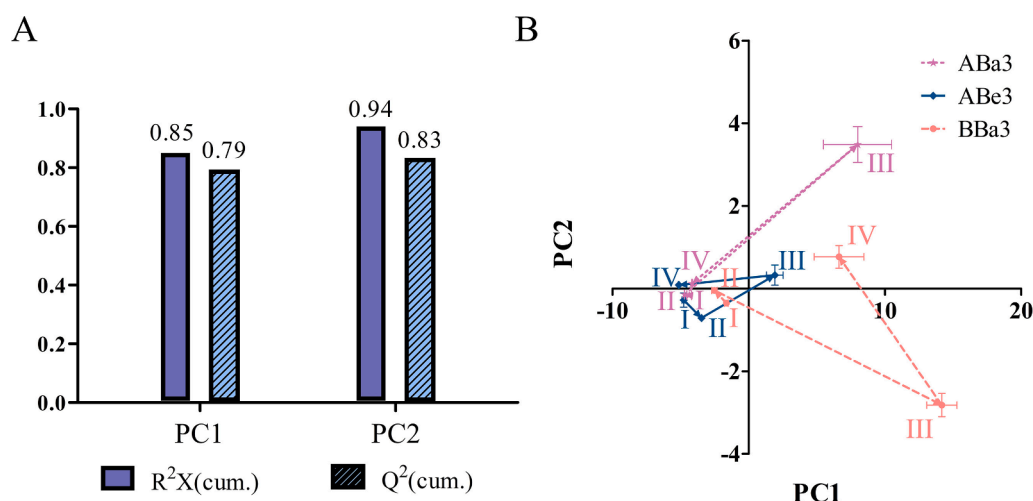


Fig. 4. Principal component analysis (PCA) of ^1H NMR spectra of ABa3, ABe3, and BBa3 at periods I (before coating), II (0 min after coating), III (3 h after coating), and IV (24 h after coating). Note: coating: coating of NCEO-FG (nanoemulsified clove essential oil and fish gelatin); ABa3: *Pseudomonas* sp. strain; ABe3: *P. psychrophila* strain; and BBa3: *P. fragi* strain.

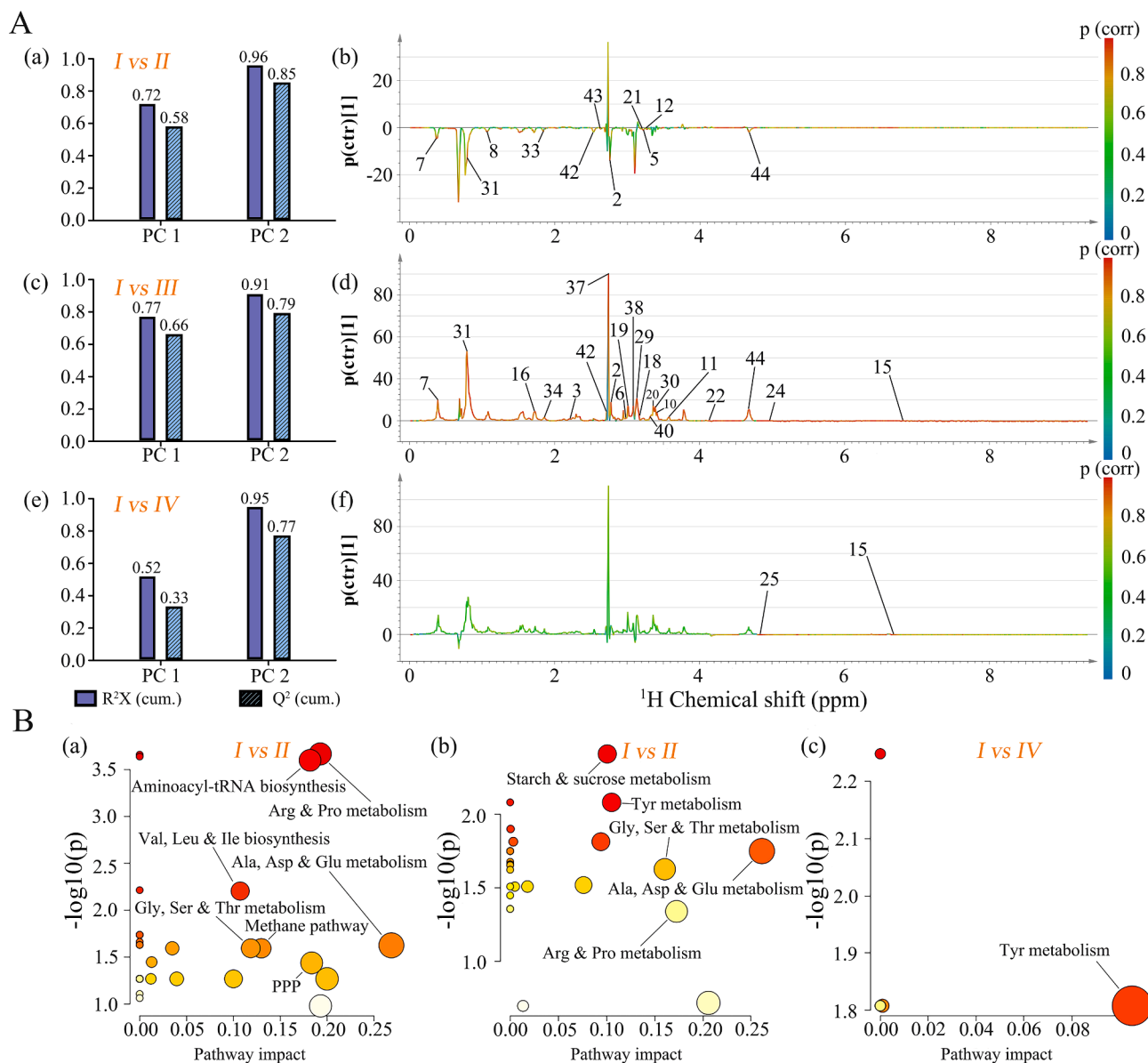


Fig. 5. Orthogonal projections to latent structures discriminant analysis (OPLS-DA) (A) and pathway analysis (B) for comparing metabolic profiles of BBa3 at periods I (before coating) with II (0 min after coating), III (3 h after coating), and IV (24 h after coating). The fitness scores (a, c, and e) and S-line (b, d, and f) of OPLS-DA. Note: coating: coating of NCEO-FG (nanoemulsified clove essential oil and fish gelatin); BBa3: *P. fragi* strain.

pursue survival in a stressful environment were discussed as follows.

3.6.1. Regulation of amino acids

Amino acids related metabolisms were susceptible to external stress (Chen et al., 2020; Wu et al., 2021), which matched well with the results of this work. After coating (II), amino acids that were identified as important in 3 strains suffered significant depletion (Fig. 6), which might be resulted from the formation of universal stress proteins (Usp). Usp, which helps bacteria cells to defeat external stresses (Matarredona, Camacho, Zafrilla, Bonete, & Esclapez, 2020), was found widely in *Pseudomonas* spp. For an instance, to defeat the toxicity of phenol, *P. putida* KT2440 upregulated the biosynthesis of 67 proteins, which were involved in functions like the general stress response, energy metabolism, and cell membrane biosynthesis (Santos, Benndorf, & Sá-Correia, 2004). Other Usp (e.g., PA3309 and PA4352) was also reported to sustain the anaerobic survival of *P. aeruginosa* (Boes, Schreiber, Härtig, Jaensch, & Schobert, 2006; Schreiber et al., 2006).

However, remarkable accumulations of amino acids were observed

after 3 h (III), which could be caused by two reasons. On the one hand, proteins that inevitably suffered denaturation and aggregation after NCEO-FG treatment needed to be eliminated to sustain cellular homeostasis (Tyedmers, Mogk, & Bukau, 2010). Therefore, those undesirable proteins were degraded by proteases into amino acids that could be utilized again (Jozefczuk et al., 2010). On the other hand, some amino acids were crucial in cells protection thus their biosynthesis was upregulated. For example, amino acids like Val, Pro, and Gly were natural osmoprotectants that could protect cellular constituents (e.g., cytoplasm and macromolecules) and sustain normal physiology (Milner, McClellan, & Wood, 1987; Zhao et al., 2020). The ones like Arg and Asp could be the alternative carbon sources in bacteria cells as they could enter the TCA cycle and produce energy after being metabolized.

No significant difference existed in the amino acid levels after 24 h (IV), which suggested the bacteria cells could gradually tolerate the NCEO-FG. In short, precise regulation of amino acids could be a practical strategy for *Pseudomonas* spp. to survive on NCEO-FG coated fillets.

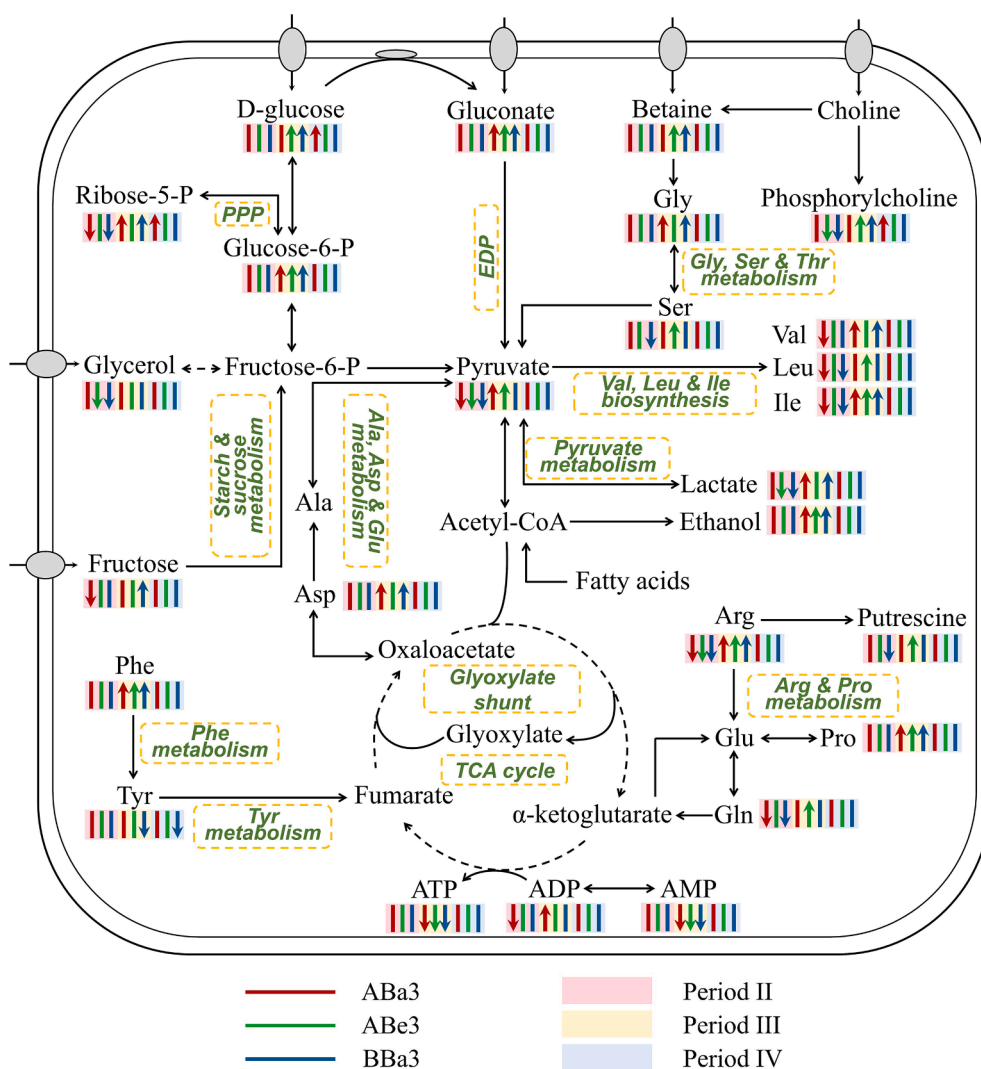


Fig. 6. The alternations of important metabolites of ABA3, ABE3, and BBa3 on NCEO-FG coated tilapia fillets at periods II (0 min after coating), III (3 h after coating), and IV (24 h after coating) compared to the period I (before coating). No arrow: no significant change in concentrations; arrow up: significant increase in concentrations; arrow down: significant reduction in concentrations. Note: coating: coating of NCEO-FG (nano-emulsified clove essential oil and fish gelatin); ABA3: *Pseudomonas* sp. strain; ABE3: *P. psychrophila* strain; and BBa3: *P. fragi* strain.

3.6.2. Alteration of energy-associated pathways

As for *Pseudomonas* species, glucose and gluconate were converted into pyruvate via the Entner–Doudoroff pathway (EDP) and then enrolled in the TCA cycle to produce energy (Kolbeck, Abele, Hilgarth, & Vogel, 2021). The second surviving strategy for *Pseudomonas* cells was related to energy metabolism.

Pyruvate, the crucial intermediate of glycolysis, suffered significant depletion immediately after coating (II), which suggested that the glycolytic pathways were susceptible to external stresses (Zhao et al., 2020). Therefore, *Pseudomonas* spp. turned to other alternative carbon sources to maintain cellular homeostasis. For example, glycerol could sustain the carbon homeostasis after being metabolized into glycolytic precursor like DHAP (Poblete-Castro, Wittmann, & Nikel, 2020). Arg and Gln were quickly converted and then entered the TCA cycle for energy production.

However, the inhibition of ATPase activity was enhanced because of the continuous sanitizing effect brought by NCEO-FG (Gill & Holley, 2006), which was confirmed by the significant reductions of ATP levels in three strains at 3 h (III). Pyruvate was no longer converted to acetyl-CoA and thus being accumulated in cells. Meanwhile, the accumulations of lactate and ethanol were observed in three strains, which suggested bacteria cells shifted to anaerobic respiration to defeat the oxidative stress. Picone et al. (2013) and Zhao et al. (2020) reported similar results before as well. At this time, the growth of bacteria cells was highly restricted. To sustain the basic cellular activity, acetyl-CoA that was

derived from fatty acids entered the glyoxylate shunt (GS) instead of the TCA cycle to produce ATP with lower requirements of oxygen and enzymes (Ahn, Jung, Jang, Madsen, & Park, 2016). Moreover, the pentose phosphate pathway (PPP) was favored when against oxidative stress as it could produce nucleotides precursors that could further assist DNA repair (Zhang, Liu, & Wong, 2003). Similar metabolic alternations were also reported in other *Pseudomonas* species. For example, when exposing to H₂O₂-induced oxidative stress, the metabolic fluxes in *P. putida* were reconfigured: the glycolysis was downregulated, but PPP was favored because it could produce NADPH that counteracted the cellular accumulation of ROS (Nikel et al., 2021).

At 24 h (IV), energy metabolism showed no obvious difference anymore, which suggested the strains could tolerate the stressful environment. In short, the alternation of the energy-associated pathways could be the second strategy.

3.6.3. Other metabolic adaptations

Other metabolic adaptations were also found in *Pseudomonas* spp. to sustain cell morphology. As a crucial precursor of phospholipids, phosphorylcholine played important role in maintaining the normal function of the cellular membrane (Wang et al., 2022). As can be discerned from Fig. 1 and Fig. 6, NCEO was able to injure the membrane integrity, which was coincident with the depletion of phosphorylcholine identified immediately after coating (II). However, the level of phosphorylcholine was then upregulated at 3 h (III), which suggested the cellular structure

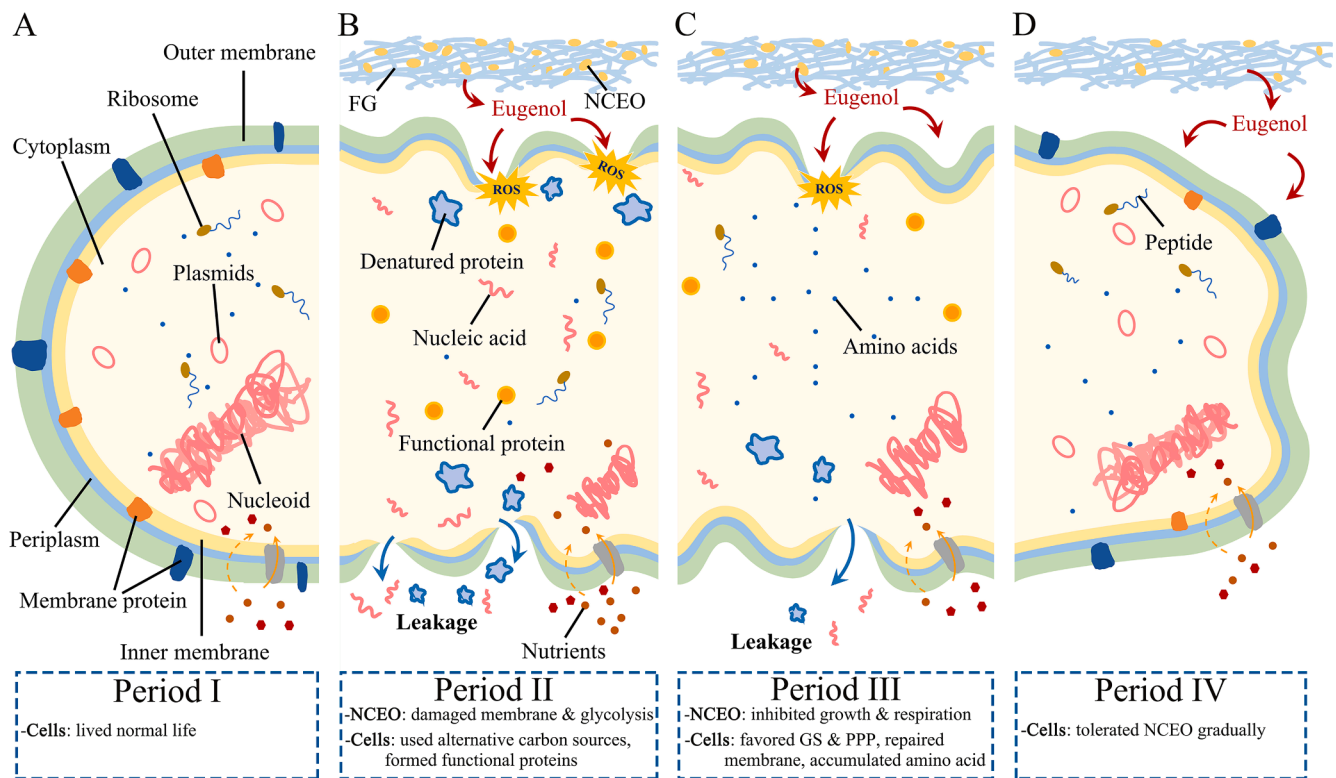


Fig. 7. The schematic diagram of NCEO-FG working mechanism and bacteria metabolic responses at periods I (before coating), II (0 min after coating), III (3 h after coating), and IV (24 h after coating) of ABA3, ABe3, and BBa3. Note: coating: coating of NCEO-FG (nanoemulsified clove essential oil and fish gelatin); ABA3: *Pseudomonas* sp. strain; ABe3: *P. psychrophila* strain; and BBa3: *P. fragi* strain.

got repaired gradually.

Osmoregulation was another method for bacteria cells against oxidative damage. Chen et al. (2010) identified a specific transporter that showed a high affinity with choline, betaine, and carnitine, which endows *Pseudomonas* spp. to effectively intake these osmoprotectants to regulate the osmotic pressure. Moreover, the accumulation of betaine had already been confirmed to sustain osmotic pressure in various bacteria like *E. coli* (von Weyarn, Nyyssölä, Reinikainen, Leisola, & Ojamo, 2001) and *P. protegens* (Tang et al., 2020). Therefore, the accumulation of betaine at 3 h suggested that *Pseudomonas* spp. tried to restore the cell morphology.

In short, to restore the cellular activity, *Pseudomonas* spp. gradually developed a defense system within 24 h, which could be summarized as follows: (i) functional proteins were formed immediately to defeat the oxidative stress brought by NCEO-FG; (ii) other alternative carbon sources (e.g., amino acids and fatty acids) were utilized to supply energy; (iii) osmotic protection was enhanced through the accumulation of amino acids and betaine; (iv) cell wall-associated compounds like phosphorylcholine were formed to repair the damaged membrane.

4. Conclusion

In this study, we confirmed that NCEO-FG coating was a promising method to effectively control the deterioration of fish meat and the growth of *Pseudomonas* spp.. With the help of NMR, the sanitizing mechanism of NCEO-FG was elucidated that it could damage the cell membrane and disturb the metabolic activities of bacteria cells. To restore the cellular activity, *Pseudomonas* spp. gradually developed a defense system relying on altering metabolisms of amino acids and energy. Overall, this report systematically elucidated the defense system launched in *Pseudomonas* spp. to respond to external stresses. Moreover, although the relationship between this defense system and drug resistance still needs more investigation, more caution should be paid when

further using the EOs in the food industry.

CRediT authorship contribution statement

Yaowen Hai: Conceptualization, Methodology, Investigation, Software, Visualization, Writing – original draft, Writing – review & editing. **Disheng Zhou:** Software, Visualization, Writing – original draft, Writing – review & editing. **Yi Lin Nicole Lam:** Investigation. **Xuan Li:** Investigation. **Guo Chen:** Investigation. **Jintian Bi:** Investigation. **Xiaowei Lou:** Methodology. **Leijian Chen:** Methodology. **Hongshun Yang:** Conceptualization, Funding acquisition, Project administration, Supervision, Writing – review & editing.

Declaration of Competing Interest

The authors declare that they have no known competing financial interests or personal relationships that could have appeared to influence the work reported in this paper.

Acknowledgements

This study was funded by Applied Basic Research Project (Agricultural) Suzhou Science and Technology Planning Programme (SNG2020061), Singapore Ministry of Education Academic Research Fund Tier 1 (21-0074-A0001) and an industry grant from Shanghai ProfLeader Biotech Co., Ltd (R-160-000-A21-597).

Appendix A. Supplementary material

Supplementary data to this article can be found online at <https://doi.org/10.1016/j.foodres.2022.111594>.

References

- Ahn, S., Jung, J., Jang, I.-A., Madsen, E. L., & Park, W. (2016). Role of glyoxylate shunt in oxidative stress response. *Journal of Biological Chemistry*, 291(22), 11928–11938.
- Baranauskienė, R., Bylaitė, E., Zukauskaitė, J., & Venskutonis, R. P. (2007). Flavor retention of peppermint (*Mentha piperita* L.) essential oil spray-dried in modified starches during encapsulation and storage. *Journal of agricultural and food chemistry*, 55(8), 3027–3036.
- Bervoets, L., Massa, G., Guedens, W., Louis, E., Noben, J.-P., & Adriaenssens, P. (2017). Metabolic profiling of type 1 diabetes mellitus in children and adolescents: A case–control study. *Diabetology & metabolic syndrome*, 9(1), 1–8.
- Boes, N., Schreiber, K., Härtig, E., Jaensch, L., & Schobert, M. (2006). The *Pseudomonas aeruginosa* universal stress protein PA4352 is essential for surviving anaerobic energy stress. *Journal of bacteriology*, 188(18), 6529–6538.
- Caldera, L., Franzetti, L. v., Van Coillie, E., De Vos, P., Stragier, P., De Block, J., & Heyndrickx, M. (2016). Identification, enzymatic spoilage characterization and proteolytic activity quantification of *Pseudomonas* spp. isolated from different foods. *Food microbiology*, 54, 142–153.
- Chen, C., Malek, A. A., Wargo, M. J., Hogan, D. A., & Beattie, G. A. (2010). The ATP-binding cassette transporter Cbc (choline/betaine/carnitine) recruits multiple substrate-binding proteins with strong specificity for distinct quaternary ammonium compounds. *Molecular microbiology*, 75(1), 29–45.
- Chen, L., Zhao, X., Li, R., & Yang, H. (2022). Integrated metabolomics and transcriptomics reveal the adaptive responses of *Salmonella enterica* serovar Typhimurium to thyme and cinnamon oils. *Food Research International*, 157, Article 111241.
- Chen, L., Zhao, X., Wu, J. E., Liu, Q., Pang, X., & Yang, H. (2020). Metabolic characterisation of eight *Escherichia coli* strains including “Big Six” and acidic responses of selected strains revealed by NMR spectroscopy. *Food Microbiology*, 88, Article 103399.
- Dahham, S. S., Tabana, Y. M., Iqbal, M. A., Ahamed, M. B., Ezzat, M. O., Majid, A. S., & Majid, A. M. (2015). The anticancer, antioxidant and antimicrobial properties of the sesquiterpene β -caryophyllene from the essential oil of *Aquilaria crassna*. *Molecules*, 20(7), 11808–11829.
- Devi, K. P., Nisha, S. A., Saktihivel, R., & Pandian, S. K. (2010). Eugenol (an essential oil of clove) acts as an antibacterial agent against *Salmonella typhi* by disrupting the cellular membrane. *Journal of ethnopharmacology*, 130(1), 107–115.
- Di Pasqua, R., Hoskins, N., Betts, G., & Mauriello, G. (2006). Changes in membrane fatty acids composition of microbial cells induced by addition of thymol, carvacrol, limonene, cinnamaldehyde, and eugenol in the growing media. *Journal of agricultural and food chemistry*, 54(7), 2745–2749.
- Ellis, D. I., & Goodacre, R. (2001). Rapid and quantitative detection of the microbial spoilage of muscle foods: Current status and future trends. *Trends in Food Science & Technology*, 12(11), 414–424.
- Feng, X., Bansal, N., & Yang, H. (2016). Fish gelatin combined with chitosan coating inhibits myofibril degradation of golden puffer (*Trachinotus blochii*) fillet during cold storage. *Food chemistry*, 200, 283–292.
- Fu, X., Gao, Y., Yan, W., Zhang, Z., Sarker, S., Yin, Y., ... Chen, J. (2022). Preparation of eugenol nanoemulsions for antibacterials activities. *RSC Advances*, 12(6), 3180–3190.
- Fu, Y., Zu, Y., Chen, L., Shi, X., Wang, Z., Sun, S., & Efferth, T. (2007). Antimicrobial activity of clove and rosemary essential oils alone and in combination. *Phytotherapy research*, 21(10), 989–994.
- Gagaoua, M., Bhattacharya, T., Lamri, M., Oz, F., Dib, A. L., Oz, E., ... Tomasevic, I. (2021). Green Coating Polymers in Meat Preservation. *Coatings*, 11(11), 1379.
- Gill, A., & Holley, R. (2006). Disruption of *Escherichia coli*, *Listeria monocytogenes* and *Lactobacillus sakei* cellular membranes by plant oil aromatics. *International Journal of Food Microbiology*, 108(1), 1–9.
- Guo, M., Zhang, L., He, Q., Arabi, S. A., Zhao, H., Chen, W., ... Liu, D. (2020). Synergistic antibacterial effects of ultrasound and thyme essential oils nanoemulsion against *Escherichia coli* O157:H7. *Ultrasonics Sonochemistry*, 66, Article 104988.
- Guo, Y., & Tao, J. (2018). Metabolomics and pathway analyses to characterize metabolic alterations in pregnant dairy cows on D 17 and D 45 after AI. *Scientific reports*, 8(1), 1–8.
- Ji, M., Wu, J., Sun, X., Guo, X., Zhu, W., Li, Q., ... Wang, S. (2021). Physical properties and bioactivities of fish gelatin films incorporated with cinnamaldehyde-loaded nanoemulsions and vitamin C. *LWT*, 135, Article 111013.
- Jozefczuk, S., Klie, S., Catchpole, G., Szymanski, J., Cuadros-Inostroza, A., Steinhäuser, D., ... Willmitzer, L. (2010). Metabolomic and transcriptomic stress response of *Escherichia coli*. *Molecular systems biology*, 6(1), 364.
- Khorshidian, N., Yousefi, M., Khanniri, E., & Mortazavian, A. M. (2018). Potential application of essential oils as antimicrobial preservatives in cheese. *Innovative Food Science & Emerging Technologies*, 45, 62–72.
- Kolbeck, S., Abele, M., Hilgarth, M., & Vogel, R. F. (2021). Comparative proteomics reveals the anaerobic lifestyle of meat-spoiling *pseudomonas* species. *Frontiers in microbiology*, 12, 695.
- Liu, X., Zhang, C., Liu, S., Gao, J., Cui, S. W., & Xia, W. (2020). Coating white shrimp (*Litopenaeus vannamei*) with edible fully deacetylated chitosan incorporated with clove essential oil and kojic acid improves preservation during cold storage. *International Journal of Biological Macromolecules*, 162, 1276–1282.
- Liu, Z., Ge, X., Lu, Y., Dong, S., Zhao, Y., & Zeng, M. (2012). Effects of chitosan molecular weight and degree of deacetylation on the properties of gelatine-based films. *Food Hydrocolloids*, 26(1), 311–317.
- Lou, X., Zhai, D., & Yang, H. (2021). Changes of metabolite profiles of fish models inoculated with *Shewanella baltica* during spoilage. *Food Control*, 123, Article 107697.
- Lv, L.-C., Huang, Q.-Y., Ding, W., Xiao, X.-H., Zhang, H.-Y., & Xiong, L.-X. (2019). Fish gelatin: The novel potential applications. *Journal of Functional Foods*, 63, Article 103581.
- Ma, Q., Zhang, Y., Critzer, F., Davidson, P. M., Zivanovic, S., & Zhong, Q. (2016). Physical, mechanical, and antimicrobial properties of chitosan films with microemulsions of cinnamon bark oil and soybean oil. *Food Hydrocolloids*, 52, 533–542.
- Marchese, A., Barbieri, R., Coppo, E., Orhan, I. E., Daglia, M., Nabavi, S. F., ... Ajami, M. (2017). Antimicrobial activity of eugenol and essential oils containing eugenol: A mechanistic viewpoint. *Critical reviews in microbiology*, 43(6), 668–689.
- Matarredona, L., Camacho, M., Zafrilla, B., Bonete, M.-J., & Esclapez, J. (2020). The role of stress proteins in haloarchaea and their adaptive response to environmental shifts. *Biomolecules*, 10(10), 1390.
- Milner, J. L., McClellan, D. J., & Wood, J. M. (1987). Factors reducing and promoting the effectiveness of proline as an osmoprotectant in *Escherichia coli* K12. *Microbiology*, 133(7), 1851–1860.
- Moghimi, R., Ghaderi, L., Rafati, H., Aliahmadi, A., & McClements, D. J. (2016). Superior antibacterial activity of nanoemulsion of *Thymus daenensis* essential oil against *E. coli*. *Food chemistry*, 194, 410–415.
- Nikel, P. I., Fuhrer, T., Chavarría, M., Sánchez-Pascuala, A., Sauer, U., & de Lorenzo, V. (2021). Reconfiguration of metabolic fluxes in *Pseudomonas putida* as a response to sub-lethal oxidative stress. *The ISME journal*, 15(6), 1751–1766.
- Nisar, T., Yang, X., Alim, A., Iqbal, M., Wang, Z.-C., & Guo, Y. (2019). Physicochemical responses and microbiological changes of bream (*Megalobrama amblycephala*) to pectin based coatings enriched with clove essential oil during refrigeration. *International Journal of Biological Macromolecules*, 124, 1156–1166.
- Ojagh, S. M., Rezaei, M., Razavi, S. H., & Hosseini, S. M. H. (2010). Effect of chitosan coatings enriched with cinnamon oil on the quality of refrigerated rainbow trout. *Food chemistry*, 120(1), 193–198.
- Picone, G., Laghi, L., Gardini, F., Lanciotti, R., Siroli, L., & Capozzi, F. (2013). Evaluation of the effect of carvacrol on the *Escherichia coli* 555 metabolome by using 1H-NMR spectroscopy. *Food chemistry*, 141(4), 4367–4374.
- Poblete-Castro, I., Wittmann, C., & Nikel, P. I. (2020). Biochemistry, genetics and biotechnology of glycerol utilization in *Pseudomonas* species. *Microbial Biotechnology*, 13(1), 32–53.
- Rezaei, F., & Shahbazi, Y. (2018). Shelf-life extension and quality attributes of sauced silver carp fillet: A comparison among direct addition, edible coating and biodegradable film. *LWT*, 87, 122–133.
- Ruttanapornvareesakul, Y., Ikeda, M., Hara, K., Osako, K., Kongpun, O., & Nozaki, Y. (2005). Effect of shrimp head protein hydrolysates on the state of water and denaturation of fish myofibrils during dehydration. *Fisheries science*, 71(1), 220–228.
- Santos, P. M., Benndorf, D., & Sá-Correia, I. (2004). Insights into *Pseudomonas putida* KT2440 response to phenol-induced stress by quantitative proteomics. *Proteomics*, 4(9), 2640–2652.
- Schreiber, K., Boes, N., Eschbach, M., Jaensch, L., Wehland, J., Bjarnsholt, T., ... Schobert, M. (2006). Anaerobic survival of *Pseudomonas aeruginosa* by pyruvate fermentation requires an Usp-type stress protein. *Journal of bacteriology*, 188(2), 659–668.
- Secci, G., & Parisi, G. (2016). From farm to fork: Lipid oxidation in fish products. A review. *Italian Journal of Animal Science*, 15(1), 124–136.
- Sessa, M., Ferrari, G., & Donsi, F. (2015). Novel edible coating containing essential oil nanoemulsions to prolong the shelf life of vegetable products. *Chemical Engineering Transactions*, 43, 55–60.
- Sheng, L., & Wang, L. (2021). The microbial safety of fish and fish products: Recent advances in understanding its significance, contamination sources, and control strategies. *Comprehensive Reviews in Food Science and Food Safety*, 20(1), 738–786.
- Shokri, S., Parastouei, K., Taghdir, M., & Abbaszadeh, S. (2020). Application an edible active coating based on chitosan-*Ferulago angulata* essential oil nanoemulsion to shelf life extension of Rainbow trout fillets stored at 4 °C. *International Journal of Biological Macromolecules*, 153, 846–854.
- Sobieszczkańska, N., Myszka, K., Szwengiel, A., Majcher, M., Grygier, A., & Wolko, L. (2020). Tarragon essential oil as a source of bioactive compounds with anti-quorum sensing and anti-proteolytic activity against *Pseudomonas* spp. isolated from fish-in vitro, in silico and in situ approaches. *International Journal of Food Microbiology*, 331, Article 108732.
- Sterniša, M., Klančnik, A., & Smole Možina, S. (2019). Spoilage *Pseudomonas* biofilm with *Escherichia coli* protection in fish meat at 5 °C. *Journal of the Science of Food and Agriculture*, 99(10), 4635–4641.
- Taliadourou, D., Papadopoulos, V., Dombvridou, E., Savvaidis, I. N., & Kontominas, M. G. (2003). Microbiological, chemical and sensory changes of whole and filleted Mediterranean aquacultured sea bass (*Dicentrarchus labrax*) stored in ice. *Journal of the Science of Food and Agriculture*, 83(13), 1373–1379.
- Tang, D., Wang, X., Wang, J., Wang, M., Wang, Y., & Wang, W. (2020). Choline–betaine pathway contributes to hyperosmotic stress and subsequent lethal stress resistance in *Pseudomonas protegens* SN15-2. *Journal of Biosciences*, 45(1), 1–10.
- Tyedmers, J., Mogk, A., & Bukau, B. (2010). Cellular strategies for controlling protein aggregation. *Nature reviews Molecular cell biology*, 11(11), 777–788.
- Vieira, B. B., Mafra, J. F., da Rocha Bispo, A. S., Ferreira, M. A., de Lima Silva, F., Rodrigues, A. V. N., & Evangelista-Barreto, N. S. (2019). Combination of chitosan coating and clove essential oil reduces lipid oxidation and microbial growth in frozen stored tambaqui (*Colossoma macropomum*) fillets. *LWT*, 116, Article 108546.
- Vital, A. C. P., Guerrero, A., Ornaghi, M. G., Kempinski, E. M. B. C., Sary, C., Monteschio, J. d. O., Matumoto-Pintro, P. T., Ribeiro, R. P., & do Prado, I. N. (2018). Quality and sensory acceptability of fish fillet (*Oreochromis niloticus*) with alginate-based coating containing essential oils. *Journal of food science and technology*, 55(12), 4945–4955.

- von Weymarn, N., Nyssölä, A., Reinikainen, T., Leisola, M., & Ojamo, H. (2001). Improved osmotolerance of recombinant *Escherichia coli* by de novo glycine betaine biosynthesis. *Applied microbiology and biotechnology*, 55(2), 214–218.
- Wang, Y., Wu, J.e., & Yang, H. (2022). Comparison of the metabolic responses of eight *Escherichia coli* strains including the “big six” in pea sprouts to low concentration electrolysed water by NMR spectroscopy. *Food Control*, 131, Article 108458.
- Wu, H., Richards, M. P., & Undeland, I. (2022). Lipid oxidation and antioxidant delivery systems in muscle food. *Comprehensive Reviews in Food Science and Food Safety*.
- Wu, J., Sun, X., Guo, X., Ge, S., & Zhang, Q. (2017). Physicochemical properties, antimicrobial activity and oil release of fish gelatin films incorporated with cinnamon essential oil. *Aquaculture and Fisheries*, 2(4), 185–192.
- Wu, J., Zhao, L., Lai, S., & Yang, H. (2021). NMR-based metabolomic investigation of antimicrobial mechanism of electrolysed water combined with moderate heat treatment against *Listeria monocytogenes* on salmon. *Food Control*, 125, Article 107974.
- Ye, Y., Zhang, L., Hao, F., Zhang, J., Wang, Y., & Tang, H. (2012). Global metabolomic responses of *Escherichia coli* to heat stress. *Journal of proteome research*, 11(4), 2559–2566.
- Yu, D., Regenstein, J. M., Zang, J., Xia, W., Xu, Y., Jiang, Q., & Yang, F. (2018). Inhibitory effects of chitosan-based coatings on endogenous enzyme activities, proteolytic degradation and texture softening of grass carp (*Ctenopharyngodon idellus*) fillets stored at 4 C. *Food chemistry*, 262, 1–6.
- Zhang, Y. M., Liu, J. K., & Wong, T. Y. (2003). The DNA excision repair system of the highly radioresistant bacterium *Deinococcus radiodurans* is facilitated by the pentose phosphate pathway. *Molecular microbiology*, 48(5), 1317–1323.
- Zhao, X., Chen, L., Wu, J.e., He, Y., & Yang, H. (2020). Elucidating antimicrobial mechanism of nisin and grape seed extract against *Listeria monocytogenes* in broth and on shrimp through NMR-based metabolomics approach. *International Journal of Food Microbiology*, 319, Article 108494.